Research Article

Variation of soil aggregates in response to soil water under short-term natural rainfalls at different land use

Yangbo He[1] · Cheng Xu[1] · Rui Huang[1] · Mingxian Guo[1] · Lirong Lin[1] · Yuanfen Yu[1] · Yao Wang[1]

Abstract

The red soils of China, South America, and Africa are highly weathered inherently infertile soils that have high erosion risks and low soil organic carbon levels. In an effort to protect these soils, they are being converted from annual crops to woodlands in China. However, under such a land use change, soil aggregate stability variation (a key factor of soil erosion) to short-term rainfall events is not clear. The objective of this study was to investigate the influence of rainfall type, soil water contents, and vegetation on short-term changes in the aggregate stability of red soils. Surface (0–20 cm) aggregate stability, SWC and dynamics (Δθ) (differences of SWC on the sampling day and prior to the sampling), rainfall, and plant root distribution (0–60 cm) were monitored from 2017 to 2018 under fir (*Taxodiaceae*), rapeseed (*Bassica napus*) and *Osmanthus fragrans* land use. The results demonstrated that the aggregate size distribution and aggregate mean weight diameter were impacted by the soil water content prior to the precipitation and plant species. Plants such as fir, lowered the soil water content which improved short-term aggregate stability. Variation of aggregate under each type of rainfall was attributed to different change of SWC among plants, which was further confirmed by significantly negative relationships between aggregate fractions (< 0.5 mm) and SWC (θ_0 and $\theta_{0.5}$, on the sampling time and half day prior to sampling) under all plants. Differences of aggregates as influenced by SWC among plants was also attributed to different plant root distribution and relative root absorption of soil water rate ($RASW_r$) [*r* between SWC and root percentage (d = 1–3 mm) was 0.99]. The study suggested that plant types should be carefully selected for their ability to protect the soil and the findings will also provide a theoretical basis for land restoration.

Keywords Aggregate · Soil water · Rainfall · Plant roots · Land use

1 Introduction

Soil aggregate stability is a key property that affects the water storage, soil aeration, crop production, and soil erosion [2]. Red soils (Ultisols) are highly weathered, low organic matter soil with low native soil fertility. The dominant clays found in these soils are kaolinite, and they are found in Africa, South America and the subtropical regions of China [39]. The soil structure of these soils has a high proportion of microaggregates due to relatively low organic matter content [13, 40]. The large number of microaggregates makes these soils susceptible to high erosion when left uncovered [12, 20, 29, 32].

Soil aggregate stability is influenced by many factors and can be impacted by seasonal and vegetation changes [9, 13]. As a response to changes in soil water retention, water infiltration, and soil organic matter aggregate stability can vary over the short and a long-term seasonal scales [5, 10, 21, 36]. Short-term changes can occur during a rainfall while long-term changes can occur across seasons or decades.

Electronic supplementary material The online version of this article (https://doi.org/10.1007/s42452-019-0934-1) contains supplementary material, which is available to authorized users.

✉ Yangbo He, kathy@mail.hzau.edu.cn | [1]Key Laboratory of Arable Land Conservation (Middle and Lower Reaches of the Yangtze River), Ministry of Agriculture, Huazhong Agricultural University, Wuhan 430070, Hubei, China.

SN Applied Sciences (2019) 1:941 | https://doi.org/10.1007/s42452-019-0934-1

Received: 5 April 2019 / Accepted: 16 July 2019 / Published online: 30 July 2019

Some studies attributed the aggregate stability variation to changes in soil organic carbon (SOC) stock under different land uses [36]. However, these changes may occur very slowly in tropical and subtropical climates [3]. Other studies suggested that soil aggregate dynamics corresponded to the variations of soil water properties [10, 21]. For example, short-term decreases in soil water content (SWC) increased soil aggregate stability on bare soil [1]. The SWC dynamics (wetting–drying cycles, wetting directions) [22, 27], and soil water infiltration [19] also influenced aggregate pore size distribution. However, SWC properties and aggregate stability can become complicated when plants are introduced into the soil.

The pattern of soil water content properties and aggregate stability varied after land use change, which depended on the impact of plants [34]. For example, Leite et al. [18] reported that soil aggregate stability was improved by switching from an annual crop to a forest. However, an opposite pattern of aggregate stability was found after reforestation from a cropland in semiarid areas, where the aggregate stability declined and the risk of soil erosion increased [20]. Differences of the relationship between aggregate stability and SWC in these studies might be attributed to the different impact of plants on soil water repellency and rainfall interception. First, plant litters (methoxyl C) and root exudate affected aggregate stability by decreasing the aggregate wetting rate due to high water repellency [6]. In addition, plants protect the soil surface by reducing splash erosion [7]. But the influence of SWC change rate under rainfall on aggregate stability was often neglected, even though [14] reported that soil aggregation breakdown was initiated through changes in SWC.

According to the aforementioned information, different pattern of SWC might occur under different rainfalls and vegetation types, however, their effect on short-term aggregate stability is not clear. Therefore, we hypothesize that transitioning from an annual cropped system to a woodland would increase soil aggregates stability. The objective of this study was to investigate the mechanism of aggregate variations in response to SWC under different short-term rainfall events under different plants (fir and *Osmanthus fragrans* woodlands transformed from cropland and croplands planted with rapeseed). The results will be effective to control soil and water erosion in ecological restoration projects.

2 Materials and methods

2.1 Study sites and soil description

The research site is located in Xianning County, southeast of Hubei province China. The mean annual temperature in the local region was approximately 16.8 °C and the mean annual precipitation was approximately 1300 mm, with more than 50% of the annual rainfall being received from March to August. Previously to 2004 the study area was mainly dominated by croplands. After that, many croplands were converted to woodland because rural exodus produced in the 90s. Three types of lands were selected in the research site (Fig. 1): (1) rapeseed (*Brassica campestris* L.) land had an area of 503 m^2, and the rapeseed grew from early October to mid of May in the following year with the rest time for fallow; (2) 13-year old fir (*Taxodiaceae*) woodland (conversion from 2005) had an area of 1386 m^2; (3) 7-year old *Osmanthus fragrans* woodland (conversion from 2010) had an area of 536 m^2.

The soil in the research site was a red soil which developed from the Quaternary red clay and was classified as Ultisols using the U. S. Soil Taxonomy system. Soil samples at 0–20 cm were collected under each plant type in fields in Oct. 2016 for basic soil characteristics analysis before the start of study (Table 1).

2.2 Soil aggregate collection and measurement

Soil aggregate samples under each plant type were collected within a range of 2 m in diameter around the position where the soil moisture probes were installed. At least three aggregate samples were collected from a depth of 0–20 cm for each field. The aggregate samples were collected before rainfall, during rainfall and after small (0.0–10 mm day^{-1}), medium (10.1–25 mm day^{-1}), large (25.1–50 mm day^{-1}), and storm (> 50.1 mm day^{-1}) precipitation events (Table 2). The rainfall events were classified according to Precipitation Level-National Standard (GB/T 28592-2012).

Aggregate samples were kept in boxes, air-dried and broken along natural cracks for use. Aggregate samples were dry-sieved through a series of sieves (5, 2, 1, 0.5, 0.25, and 0.1 mm) to obtain each fraction of dry aggregate. Soil aggregate samples were also divided into subsamples to measure the wet aggregate stability by following the method in Le Bissonnais [17]. 10 g of soil aggregates (2–5 mm) were oven-dried at 40 °C for about 24 h to a constant weight for subsequent wet-sieving aggregate analysis. The aggregate water stability was determined by the fast wetting method using an aggregate analyzer (XY-100, Beijing) for 5 min (amplitude 2 cm, 20 oscillations min^{-1}) following the method of Le Bissonnais [17]. The mean weight diameter (MWD_{fw}) and the relative slaking index (RSI) were defined as shown in Eqs. 1 and 2.

$$MWD = \sum_{i=1}^{n+1} \frac{r_{i-1} + r_i}{2} \times m_i \tag{1}$$

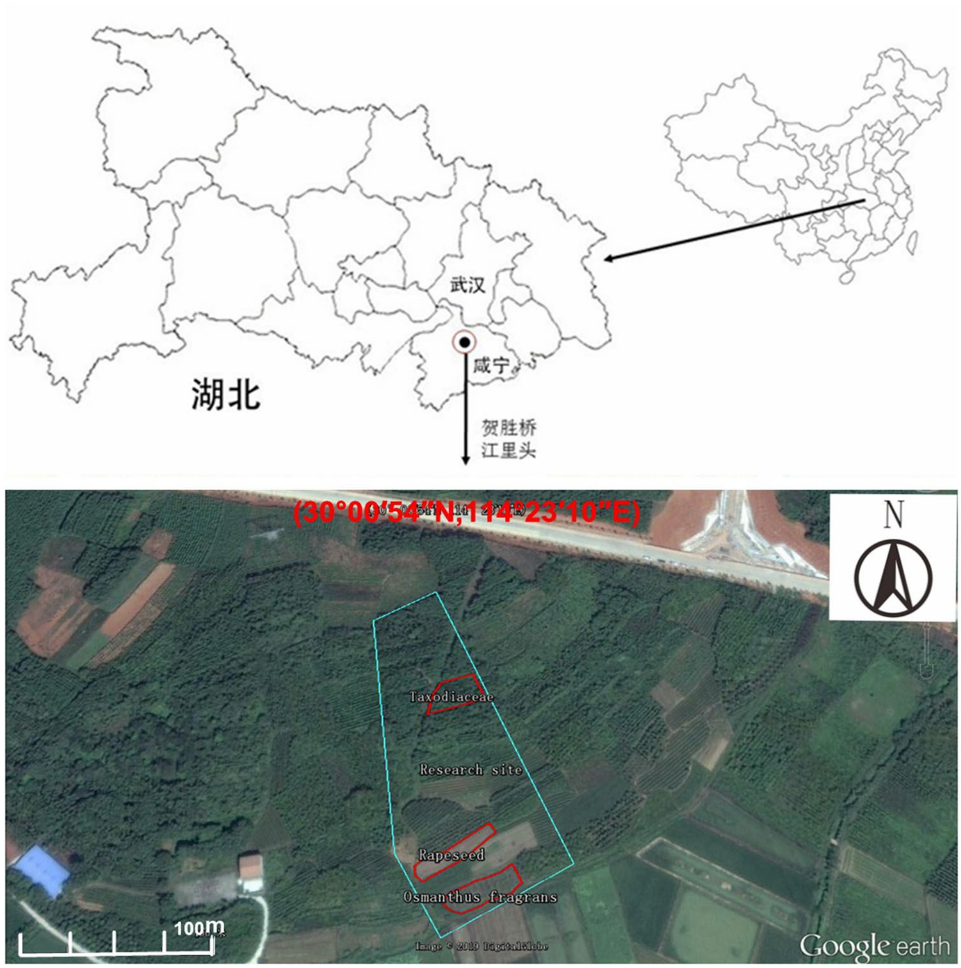

Fig. 1 Schematic diagram of the research site land use

where r = aperture of the ith mesh (mm), $r_0 = r_1$, and $r_n = r_{n+1;}$ m_i = mass fraction of aggregates remaining on ith sieve; n = number of sieves. The results of the test for fast wetting were refereed as MWD_{fw}.

$$RSI = \frac{MWD_{SW} - MWD_{FW}}{MWD_{SW}} \times 100 \quad (2)$$

where MWD_{SW} and MWD_{FW} are the MWD in the treatment of slow wetting and fast wetting methods, respectively.

2.3 Soil water content measurement

The volumetric SWC measurement in all fields was monitored from Nov. 2016 to June 2018 to display the variation of SWC. In Oct. 2016, moisture probes (Decagon Devices Inc., Pullman, WA) were installed in the middle of each field and were connected to a datalogger (Watchdog 2400, Spectrum Technologies, Inc.). The moisture probes were installed to different depths, but only 0–20 cm SWC data in a frequency of 30 min was used in this study. Before the sensors were installed, calibrations were conducted. SWC variations across five different rainfall events were displayed by coefficient of variation (CV). Further SWC conditions were expressed by two indices which included the mean SWC for a duration t (in days) prior to the soil aggregate sampling (θ_t) and the differences in SWC between the beginning and the end of that period ($\Delta\theta_t$). In this study, θ_0 (at the sampling day), $\theta_{0.5}$ (half day prior to sampling), θ_2, θ_4, $\Delta\theta_{0.5}$, $\Delta\theta_2$, and $\Delta\theta_4$ were also analyzed. Meteorological data were obtained from a weather station 1.5 km from the study site. A separate rainfall gauge was installed under the fir field to monitor difference of the amount of rainfall under trees and the bare field.

2.4 Plant root analysis

To measure the water uptake ability of plants, the root distributions of different types of plants were determined in April 2016 and Aug. 2017. Roots were taken to a soil depth of 0–20, 20–40, and 40–60 cm using cores (200 cm^3) for fir and *Osmanthus fragrans* fields at the position of 25 cm and 50 cm to the base of trees. Rapeseed roots were also taken to soil depth of 0–20, 20–40, and 40–60 cm at a point with row distance of 25 cm. Roots were washed by water, stored in − 20 °C refrigerator and scanned by the LA2400 Scanner for images (Regent instruments Canada Inc.) [28]. After that, root length and diameter were analyzed by WinRhizo, and root length density (RLD) was calculated. Finally, relative root absorption of soil water rate ($RASW_r$) was calculated based on the relative absorption of soil water (RASW) as in Eq. 4 [38].

$$RASW_{(z)} = \frac{\theta_{actual} - \theta_{pw}}{\theta_{fc} - \theta_{pw}} \quad (3)$$

$$RASW_{r(z)} = RASW_{(z)} \times \frac{RLD_z}{RLD\text{max}} \quad (4)$$

where z was a certain soil depth, θ_{actual} was the actual measured SWC by moisture probe, θ_{pw} was the wilting point of soil, θ_{fc} was the field capacity of the soil. RLD_z/RLD_{max} was the relative root length abundance (ratio of RLD at depth of z to maximum RLD).

2.5 Statistical analysis

Soil aggregate MWD_{fw} differences with the time steps of each rainfall event for all plant types were tested using the Fisher's least significant difference (LSD) test ($p < 0.05$) in SPSS 17.0. The Pearson correlations between MWD_{fw}, rainfall duration, rainfall amount, the maximum rainfall intensity, θ_0, $\theta_{0.5}$, θ_2, θ_4, $\Delta\theta_{0.5}$, $\Delta\theta_2$, and $\Delta\theta_4$ were all performed. All the Figures were plotted by Origin 8.0.

3 Results

3.1 Short-term variation of soil aggregate stability under rainfall events

Soil MWD_{fw} varied with time under the five different rainfall events (Fig. 2). Soil MWD_{fw} dropped to a minimum value on the rainfall event day and became stable or slightly returned to the original value with time after the rainfall stopped. For example, under the large rainstorm on Aug. 2017, MWD_{fw} declined to minimum values of 0.22 mm, 0.26 mm and 0.32 mm for *Osmanthus fragrans*, rapeseed, and fir, respectively, which displayed a relative decline of 37.9% (*Osmanthus fragrans*), 38.7% (rapeseed), and 13.9% (fir) compared to their original MWD_{fw} values (Fig. 2). For the large rainfall event on Sep. 2017, MWD_{fw} displayed a similar pattern as the August large rainstorm except that the fir soil had a greater decrease (30%). MWD_{fw} exhibited a smaller degree of change with time at medium and small rainfalls. The decline pattern of MWD_{fw}

Table 1 The soil properties under different vegetation type in each site in 2016

Land use	Soil depth (cm)	Clay (%)	Silt (%)	Sand (%)	Bulk density (g cm^{-3})	Soil organic carbon (SOC) (g kg^{-1})	pH	Saturated water content (cm^3 cm^{-3})	Field capacity (cm^3 cm^{-3})	Wilting point (cm^3 cm^{-3})
Osmanthus fragrans (*Osmanthus fragrans* Lour.) (7 years old)	0–20	26.8	70.1	3.1	1.55	8.76	4.90	0.42	0.36	0.21
Rapeseed (*Brassica campestris* L.)	0–20	28.8	67.8	3.4	1.51	8.50	4.99	0.43	0.36	0.20
Fir (*Taxodiaceae*) (13 years old)	0–20	39.0	57.2	3.8	1.40	9.24	5.14	0.47	0.40	0.25

Table 2 Sampling pattern under the rainfall event and variability of the rainfall event characteristics

Date	Sampling	Rainfall event	Duration (h)	Rainfall amount (mm)	Average intensity (mm/h)	Maximum intensity (mm/h)
2017/6/5		R1	4.5	8.5	1.89	2.4
2017/6/6	S					
2017/6/8	S	R2	1.5	3.4	2.27	2.4
2017/8/11	S					
2017/8/12		R3	15.5	42.8	2.76	11.8
2017/8/13	S	R4	15	118	7.87	23.5
2017/8/17	S					
2017/9/17	S					
2017/9/19	S	R5	12	48	4	16.9
2017/9/20		R5	3	3.1	1.03	1.2
2017/9/22	S					
2017/9/26	S					
2017/10/14	S					
2017/10/16	S	R6	24	22.4	0.93	3.5
2017/10/20	S					
2018/5/17	S					
2018/5/18		R7	2	21.2	10.6	17
2018/5/20	S	R8	3.5	45.7	13.1	15.9
2018/5/21		R9	4.2	40.7	9.8	16.4
2018/5/24	S					

S soil sampling, *R* rainfall event

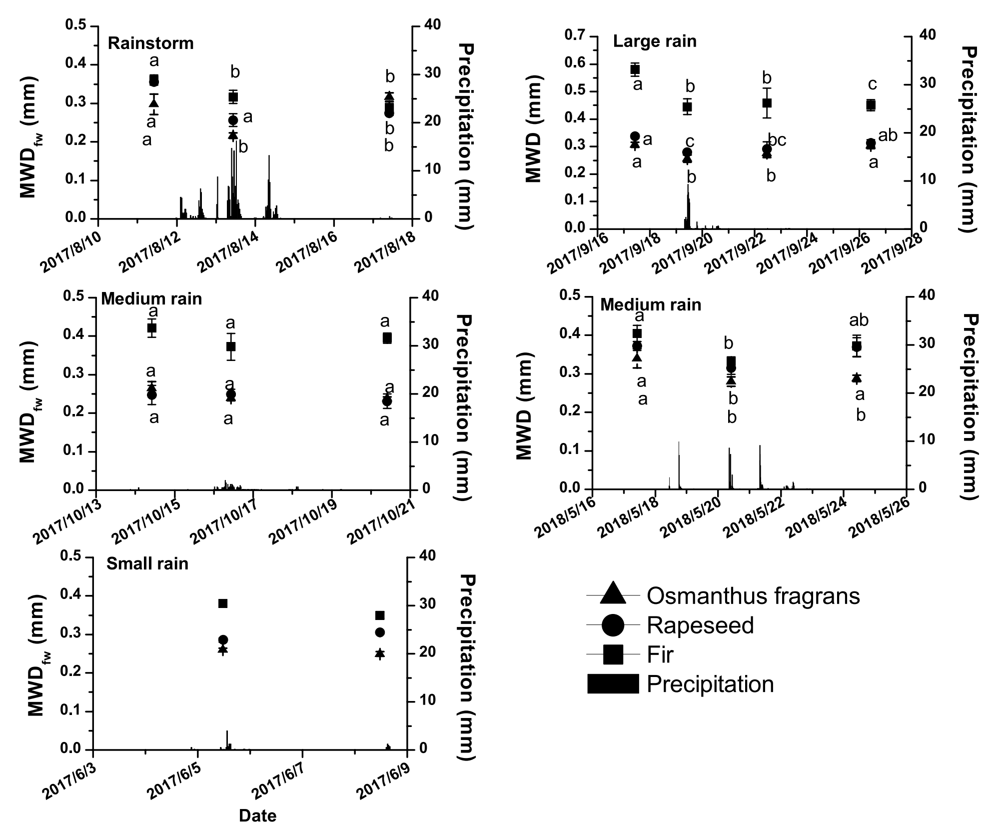

Fig. 2 Variation of aggregate MWD_{fw} with time under different rainfall events. Different lower-case letters indicate significant differences of MWD_{fw} with time steps under each plant field

with rainfall events was confirmed by the significant correlation between rainfall duration, rainfall amount, maximum rainfall intensity, and aggregate size fraction (Supplemental Table 1).

The best correlation coefficient was found between the rainfall amount and aggregate size fraction (0.5–0.25 mm) as *r* of − 0.66, − 0.91, and − 0.84 for *Osmanthus fragrans*, rapeseed, and fir, respectively (Supplemental Table 1). This indicates that rainfall amount negatively impacted macroaggregate (> 0.25 mm) after rainfalls. For example, the soil macroaggregate proportion under fir decreased from 66.5% (before rainfall: 17 Sep., 2017) to 45.5% (after rainfall: 19 Sep., 2017). Correspondingly, the microaggregate fraction significantly increased during the same period. The aggregate MWD_{fw} change with rainfall effect can be indicated by different RSI values for each plant field (Fig. 3). Significant increase of RSI with time after rainfall was in agreement with the decline pattern of MWD_{fw} with time under rainfall in Fig. 2 for all lands. MWD_{fw} change in a short-term among plant types was similar as that in a year time (Fig. 4).

3.2 Soil water dynamics with rainfall under different plants

3.2.1 Soil water content dynamics with rainfall

The SWC values also varied in response to rainfall events, which displayed an opposite trend compared to the trend of MWD_{fw} for all plants (Fig. 5). The SWC values increased sharply with the beginning of rainfall followed by a gradual decline to relatively stable values after rainfall stopped, but SWC displayed different extent of variation among rainfall types. The variation of SWC was largest in a rainstorm (i.e., rapeseed coefficient of variation (CV) = 11.1%) and the smallest in a small rainfall (CV = 0.56%). Variation of SWC in response to the rainfall event was also expressed by $\Delta\theta_{0.5}$, $\Delta\theta_2$, and $\Delta\theta_4$. Considering all these parameters, variations of SWC were also different among the land use types, with the most for rapeseed and the least for fir under the same rainfall.

3.2.2 Plant root properties relationship with SWC

Root length distribution and root length density (RLD) displayed differently within depths among the three plant types (Fig. 6) and were responsible for the difference of SWC among plants. Among the root length, root diameter < 1 mm was dominant in different plants, where rapeseed had a higher percentage (> 70%) of this type of root than fir and *Osmanthus fragrans*. However, root length (d = 1–3 mm) of rapeseed was approximately 20% lower than that the other plants. Besides, high RLD appeared at surface 20 cm of soils for all plants (Fig. 6). Such root length distribution and RLD resulted in different root relative absorption of soil water ($RASW_r$) values among soils. For example, $RASW_r$ was 41.6%, 79.1%, and 19.5% for *Osmanthus fragrans*, rapeseed, and fir,

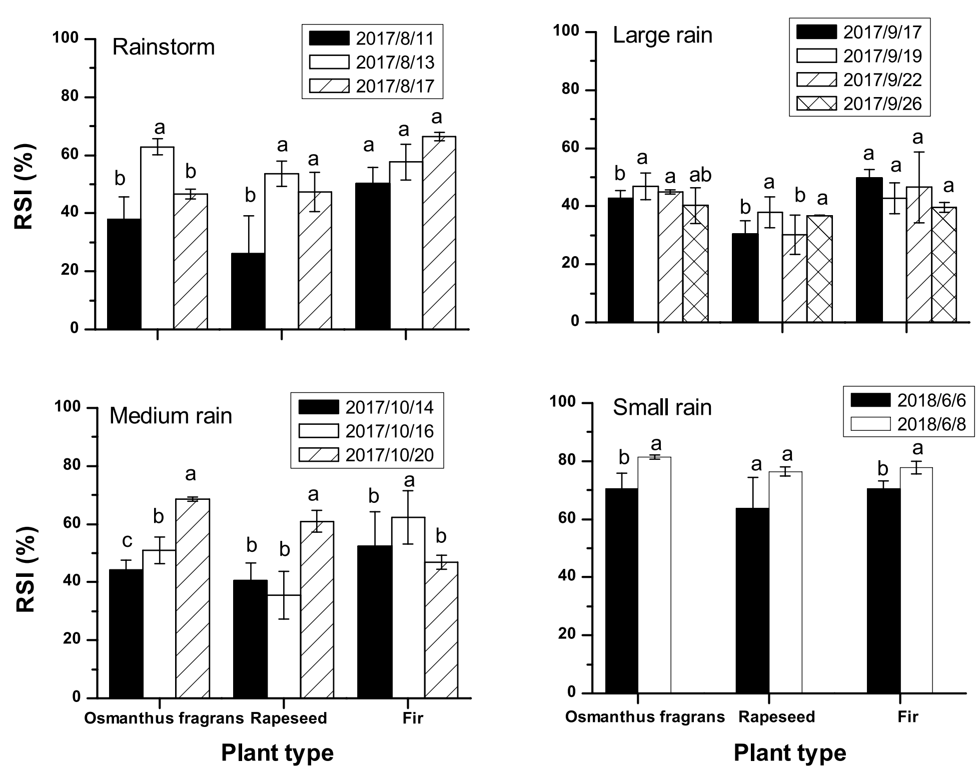

Fig. 3 Soil RSI under different rainfall events. Different lowercase letters indicate significant differences of RSI with time steps under each plant field

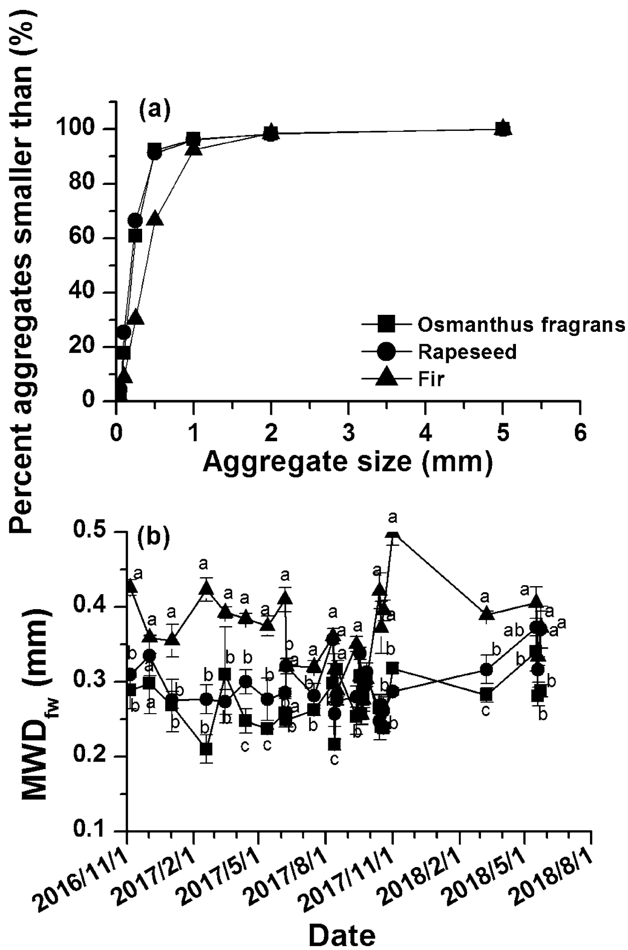

Fig. 4 Soil aggregate properties: **a** aggregate size distribution for example samples taken on 1 Nov. 2017, **b** soil MWD_{fw} comparison among the three plant types over a year time, different letters indicate significant differences of MWD_{fw} within type of plant at each time

respectively in 2017. The effect of plant root properties on SWC was especially obvious for the percentage of plant roots (d = 1–3 mm) (0–20 cm) which was indicated by a significant correlation with SWC with *r* values of 0.99 (fir), 0.99 (*Osmanthus fragrans*), and 0.63 (rapeseed) (data not shown).

3.3 Relationships between aggregate stability and soil water content

Above soil water indices including soil water content (θ) values and dynamics (Δθ) were dominant factors of soil aggregate stability, because they played different roles on aggregate fractions (Table 3). For example, θ_0 and $\theta_{0.5}$ were significantly and negatively correlated with aggregate fraction (0.5–0.25 mm) for rapeseed and *Osmanthus fragrans* lands. However, θ_0 and $\theta_{0.5}$ were significantly and positively correlated with aggregate (0.25–0.1 mm, 0.1–0.053 mm, < 0.053 mm) fraction for rapeseed and *Osmanthus fragrans* lands. Especially, $\theta_{0.5}$ was correlated with aggregate (0.5–0.25 mm%) as − 0.66 and − 0.66 for rapeseed and *Osmanthus fragrans* lands, respectively. In addition, $\Delta\theta_2$ and $\Delta\theta_4$ positively contributed to the formation of microaggregate (< 0.1 mm) for fir land, but was not significantly correlated with any of aggregate fractions for rapeseed and *Osmanthus fragrans* lands. After the variation of aggregate size distribution due to SWC, soil MWD_{fw} became different among plants.

4 Discussion

4.1 Soil aggregate varied before and after rainfall event

Temporal change in MWD_{fw} can occur over a few days, depending on rainfall and vegetation. Similar short-term change of aggregate stability (up to 46%) was also observed over a 7-days period on bare soils (0–0.5 cm) in Algayer et al. [1]. Rainfall generally played important roles in inducing aggregate destruction, soil crusting and soil loss due to throughfall kinetic energy [16], however, differences in the amplitude of aggregate change under rainfall in studies were probably associated with soil coverage. For example, in our study, rain duration and rainfall amount appeared to be the dominant factors controlling aggregate stability over all rainfall events, instead of the rain intensity in Algayer et al. [1] and Sajjadi and Mahmoodabadi [25]. The differences in studies were attributed to the different soil coverage. Study in Algayer et al. [1] was conducted on bare field where soil was more susceptible to the splash erosion from high velocity of raindrops [14]. Our present study underlined the role of plants to reduce rainfall splash effects on aggregation, for example, rainfall water that was received under fir (measured by a rainfall gauge at site) can be reduced by 28–68% compared to that on bare soils.

The change pattern of rapid decline of aggregate (MWD_{fw}) following rainfall initiation and then gradual increase following rainfall termination (drying process) was due to below mechanisms. Firstly, MWD_{fw} declined at the start of the rainfall, because it provoked a wetting process of soil with larger rainfall amount resulting in more slaking destruction of soil aggregates. This was confirmed by a decrease of aggregate (2–0.25 mm) fraction and an increase of microaggregates (< 0.25 mm) in our study, which was in agreement with [25]. Destruction of macroaggregate from rainfall effect outweighed the aggregate formation, resulting in the net decline of MWD during the rainfall day [21]. Secondly, aggregate MWD_{fw} improved again with time after rainfall stopped, and almost returned to the original value before rainfall event. At this time, the

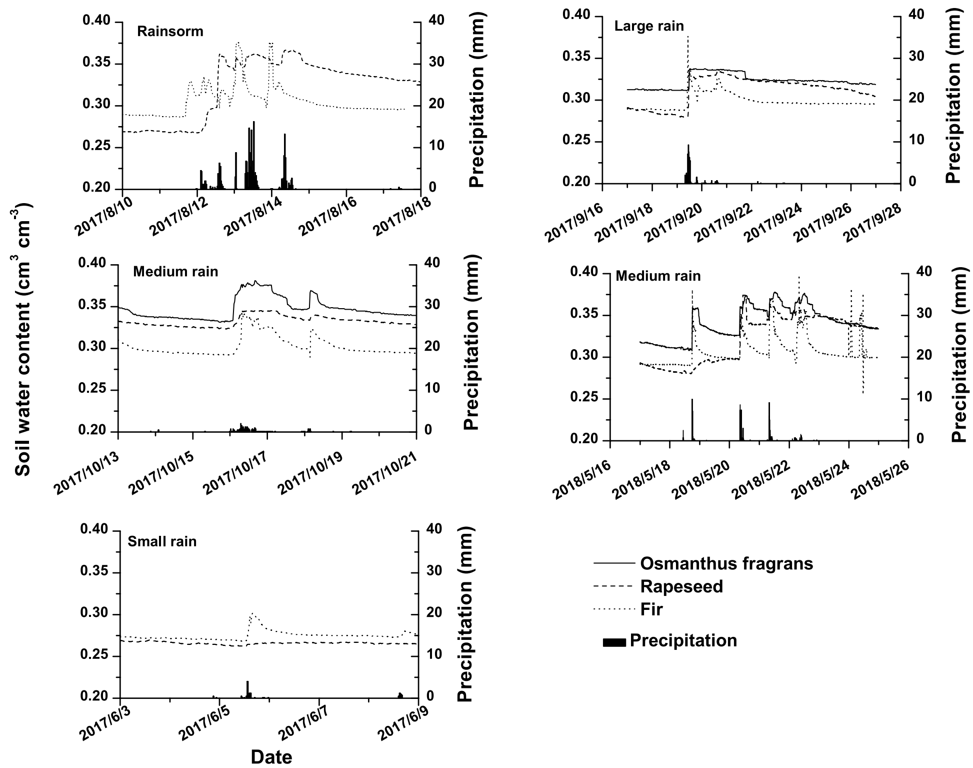

Fig. 5 Soil water content variation with time under different rainfall events

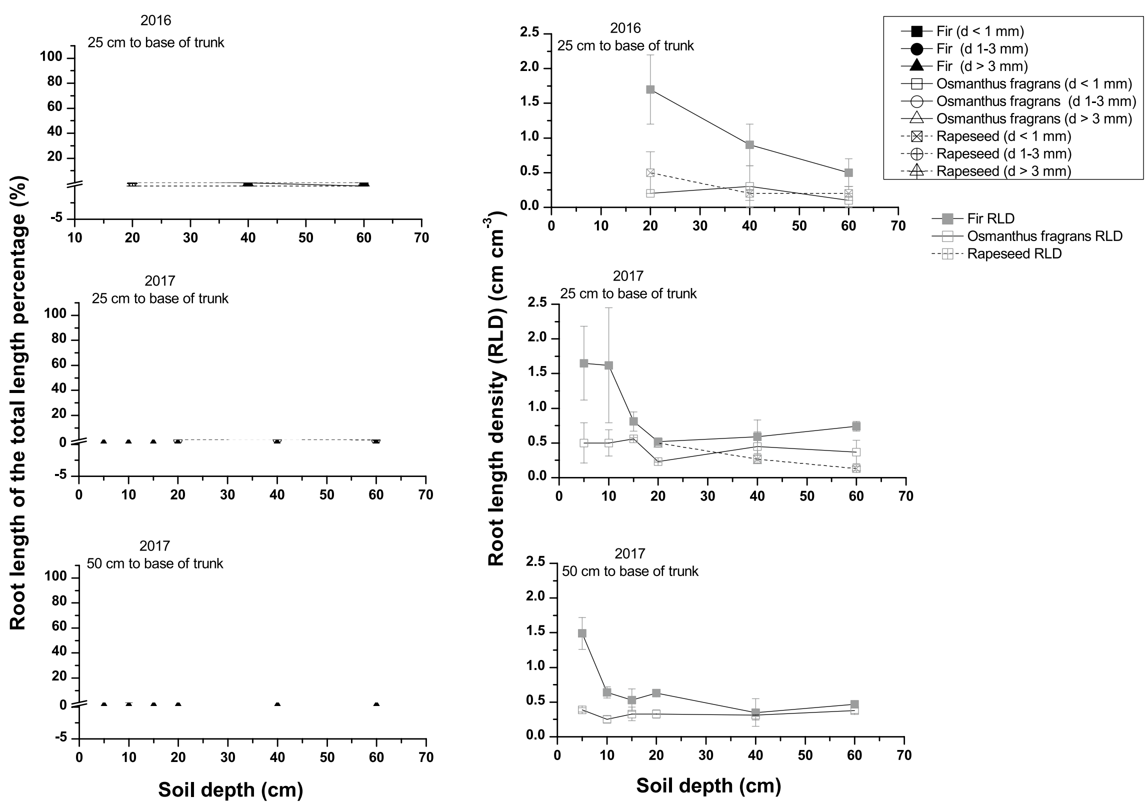

Fig. 6 Plant root length distribution and root length density (RLD) at different soil depths for three types of plants

Table 3 Correlations between aggregate parameters and soil water indices

Land use	Aggregates	θ_0^a	$\theta_{0.5}$	θ_2	θ_4	$\Delta\theta_{0.5}^b$	$\Delta\theta_2$	$\Delta\theta_4$
Rapeseed	MWD_{fw}	−0.46	−0.44	−0.25	−0.16	0.01	−0.16	−0.26
	> 2 mm%	−0.17	−0.07	0.09	0.15	0.04	0.01	−0.11
	2–1 mm%	−0.37	−0.30	−0.13	−0.06	−0.08	−0.15	−0.23
	1–0.5 mm%	−0.55*	−0.53*	−0.34	−0.25	0.11	−0.18	−0.23
	0.5–0.25 mm%	−0.62*	−0.66**	−0.47	−0.37	−0.08	−0.31	−0.37
	0.25–0.1 mm%	0.59*	0.57*	−0.15	−0.06	−0.29	−0.30	−0.10
	0.1–0.053 mm%	0.65**	0.65**	0.47	0.36	0.16	0.33	0.34
	< 0.053 mm%	0.63*	0.65**	0.44	0.30	0.14	0.37	0.36
Osmanthus fragrans	MWD_{fw}	−0.52	−0.55	0.12	0.14	−0.38	−0.05	−0.22
	> 2 mm%	−0.39	−0.39	0.23	0.30	−0.28	0.01	−0.07
	2–1 mm%	−0.20	−0.12	0.38	0.43	−0.26	0.05	0.06
	1–0.5 mm%	−0.42	−0.52	0.10	0.11	−0.23	0.07	−0.12
	0.5–0.25 mm%	−0.61*	−0.66**	−0.09	−0.12	−0.45	−0.20	−0.42
	0.25–0.1 mm%	0.60*	0.64*	0.01	−0.01	0.40	0.12	0.33
	0.1–0.053 mm%	0.61*	0.64*	0.15	0.17	0.48	0.25	0.48
	< 0.053 mm%	0.57*	0.63*	0.00	0.02	0.43	0.12	0.33
Fir	MWD_{fw}	−0.28	−0.16	−0.17	−0.24	−0.28	−0.36	−0.30
	> 2 mm%	0.03	0.19	0.15	0.09	−0.12	−0.15	−0.07
	2–1 mm%	−0.28	−0.16	−0.15	−0.18	−0.30	−0.38	−0.27
	1–0.5 mm%	−0.27	−0.20	−0.21	−0.33	−0.22	−0.27	−0.29
	0.5–0.25 mm%	−0.22	−0.34	−0.29	−0.46	−0.06	−0.28	−0.46
	0.25–0.1 mm%	0.22	0.21	0.21	0.40	0.15	0.23	0.31
	0.1–0.053 mm%	0.44	0.39	0.34	0.38	0.35	0.55*	0.53*
	< 0.053 mm%	0.37	0.27	0.25	0.25	0.34	0.53*	0.55*

[a]θ Indicates average SWC at the day of sampling (0) or certain days (0.5, 2, 4) before the day of sampling

[b]$\Delta\theta_{0.5}$ means difference of SWC at the time of sampling and at SWC 0.5 days before sampling

*Significant at α = 0.05; **significant at α = 0.01

aggregates that were dominated by particles < 0.25 mm were generally more susceptible to be released in next rainfalls to block soil pores, affecting soil permeability and surface runoff [11], and soil sensitivity to erosion [17, 31]. These results confirmed the negative effect of rainfall duration and amount on aggregate size and the positive effect of after-rainfall periods on aggregate size.

4.2 Soil aggregate as controlled by soil water content and plants

Variation of aggregate MWD_{fw} in the above rainfall events can be attributed to the significant change of SWC as adjusted by the plant types. Firstly, the significantly negative relationship between the fraction of mesoaggregate (1–0.25 mm) and SWC (θ_0 and $\theta_{0.5}$) confirmed that SWC values at the sampling time (θ_0) and half day prior to sampling time ($\theta_{0.5}$) might break the extent of the mesoaggregate (1–0.25 mm). The results were in agreement with [13] who also attributed the aggregate destruction to the antecedent SWC. When the antecedent SWC was low, the slaking was the major reason for aggregate breakdown, but when the antecedent SWC was high, non-uniform expansion of soil minerals was the dominant factor for aggregate breakdown [22]. In addition, the dynamics of SWC (Δθ) also broke mesoaggregate probably due to the wetting–drying cycle effect [22]. Moreover, dynamics of SWC as influenced by the rainfall type was responsible for different MWD_{fw} under each plant field. For example, the improvement of SWC after rainfalls resulted in the decline in aggregate stability through the loss of interparticle cohesion [26] or slaking [37]. In contrast, the decline of SWC (drying process) increased the aggregate stability due to the formation of bonds between particles [15]. Generally, the SWC had dominant effect on the soil aggregation, which was different among plant types.

Plants impacted aggregation also through modifying the SWC distribution as below approaches. Plant regulated SWC distribution through functions of interception of rainfall by vegetation coverage, absorption of water by roots, and change of water infiltration. Firstly, the canopy intercepted large amount of rainfall and reduced the SWC dynamics [7, 16]. In our study, high canopy of fir with small leaves reduced 28–68% of rainfall water compared to that on the bare soil surface, responsible for its lowest SWC variation and the highest aggregate MWD. Similar plant effect on the relationship between SWC and aggregate was reported in Linsler et al. [21] that permanent grassland soils (11 years) with low SWC in dry season resulted in high large water-stable macroaggregate proportion in surface soils, while cropland transformed from grassland with high SWC variations leaded to more aggregate destruction. Secondly, different root distribution among three plants fields also displayed different RLD and $RASW_r$ to regulate SWC regimes (*r* between RLD and SWC > 0.99). Different $RASW_r$ among plants (rapeseed > Osmanthu fragrans > fir at surface 20 cm soils), together with different plant roots exudates and litters properties probably exhibited different soil water repellency to control aggregate stability [6]. Thirdly, different soil water infiltration due to different cushions of rainwater, velocity of raindrops, and soil pore distribution, was responsible for different SWC dynamics. For example, Pan et al. [24] found that the tree cover systems with 86% of soil water infiltration coefficient caused less SWC variation than the control (68%). In our study, large fraction of small pores (< 30 μm) existed in the fir soils, while many 30–500 μm transmission pores existed in the other two soils, which may result in different magnitude of infiltration and SWC variation during wetting and drying process (Supplemental Fig S1). Generally, all these factors may explain the most intensive SWC variations under rapeseed and smallest variations under fir, and therefore, these resulted in the least MWD under rapeseed while highest MWD under fir.

Except for SWC effect on aggregation, average soil organic carbon (SOC), as a binding agent of aggregate [8], displayed no significant differences with the time of rainfall among each aggregate fraction (data not shown). Our study was different from Yu et al. [36] that reforestation increased C sequestration, which was probably because short-time land transformation was not yet effective in changing SOC in subtropical climate in our study. Hence, SOC was not the dominant factor in determining aggregate stability in short-time rainfall in our study. Besides, free Fe-oxides, as another important binding agent of aggregate in red soil [35], was significantly greater in fir field than rapeseed field (2.1 vs. 1.1 g kg^{-1}), but will be difficult to change in a few days. Therefore, soil aggregate stability was dominantly determined by above SWC properties under short-term rainfall as influenced by plant types instead of SOC and oxides.

Large rural-to-urban mitigation occurred in 60.2% of rural lands in China in 2016 [23], creating a great land use change in rural regions. Similar land use change during rural exodus was also reported in other developing countries such as Brazil, Laos, Kenya etc., influencing environmental healthy [16, 33]. During the land use change, other authors also found that the water erosion was generally lower over afforested areas [16], aggregate stability was higher in afforested areas [18], and that soil microbial biomass, microbial C, N, P increased when a similar situation was produced in a mixed forest areas in India [30]. Soil aggregate stability was inversely related with the soil erodibility index K [4]. Therefore, understanding the aggregate variation mechanism with SWC under different plant type and time of land use transformation will be important to control soil and water erosion in rainy season. But the effect of single woodland was still limited to resist the soil erosion, high coverage (tress with high canopy and small leaves) combined with minimum height of grass underneath trees was suggested to be the most effective structure to conserve soils [16].

5 Conclusions

Soil aggregate stability varied in response to SWC as influenced by short-term rainfall events at all plant fields. Variation of aggregate MWD_{fw} with SWC was due to different change of aggregate fraction and RSI under rainfall event. The SWC (θ_0 and $\theta_{0.5}$, on the sampling time and half day prior to the sampling time) was the dominant factor to determine the aggregate stability which was confirmed by the significantly negative relationship between θ_0 and $\theta_{0.5}$ and aggregate fraction (0.5–0.25 mm). Such SWC effect on aggregation with time depended on the process of rainfall and was significantly different under rainfall duration and amount. The SWC effect on aggregation was also adjusted by different plant root distribution and $RASW_r$ which was confirmed by significant correlation between SWC and plant roots percentage (d = 1–3 mm) at 0–20 cm. Generally, aggregate stability was determined by the variation of SWC, with the highest aggregate stability for fir field (least SWC variation) and the least for *Osmanthu fragrans* field (highest SWC variation). The results will provide theoretical basis during land use transformation considering the soil and water protection. Coniferous woodland will be suggested to improve the aggregate stability to prevent water erosion during ecological restoration for policymakers.

Acknowledgements This work was supported by the National Natural Science Foundation of China (41601219, 2016; 41601220, 2016), the Fundamental Research Funds for the Central Universities (Program No. 2662015BQ030, 2015), and National Natural Science Foundation of China (41601220). We are grateful to Feng Gu, Jing Song, Jiangnan Li and Zhizhang Guan for part of soil samples collection and analysis.

Compliance with ethical standards

Conflict of interest On behalf of all authors, the corresponding author states that there is no conflict of interest.

References

1. Algayer B, Le Bissonnais Y, Darboux F (2014) Short-term dynamics of soil aggregate stability in the field. Soil Sci Soc Am J 78:1168–1176
2. Amezketa E (1999) Soil aggregate stability: a review. J Sustain Agric 14:83–151
3. Attard E, Le Roux X, Charrier X, Delfosse O, Guillaumaud N, Lemaire G, Recous S (2016) Delayed and asymmetric responses of soil C pools and N fluxes to grassland/cropland conversions. Soil Biol Biochem 97:31–39
4. Barthes B, Roose E (2002) Aggregate stability as an indicator of soil susceptibility to runoff and erosion; validation at several levels. CATENA 47:133–149
5. Castiglioni MG, Sasal MC, Wilson M, Oszust JD (2018) Seasonal variation of soil aggregate stability, porosity and infiltration during a crop sequence under no tillage. Terra Latinoam 36:199–209
6. Cesarano G, Incerti G, Bonanomi G (2016) The influence of plant litter on soil water repellency: insight from C-13 NMR spectroscopy. PLoS ONE. https://doi.org/10.1371/journal.pone.0152565
7. Chen WJ, Qi KB, Huang JS, Yang TH, Bao WK, Pang XY (2017) Effect of reforestation with different tree species on soil water-holding capacity in western Sichuan province. Acta Ecol Sin 37:4998–5006 **(in Chinese)**
8. Dara A, Baumann M, Kuemmerle T, Pflugmacher D, Rabe A, Griffiths P, Hoelzel N, Kamp J, Freitag M, Hostert P (2018) Mapping the timing of cropland abandonment and recultivation in northern Kazakhstan using annual Landsat time series. Remote Sens Environ 213:49–60
9. Denef K, Six J, Bossuyt H, Frey SD, Elliott ET, Merckx R, Paustian K (2001) Influence of dry–wet cycles on the interrelationship between aggregate, particulate organic matter, and microbial community dynamics. Soil Biol Biochem 33:1599–1611
10. Dimoyiannis D (2009) Seasonal soil aggregate stability variation in relation to rainfall and temperature under Mediterranean conditions. Earth Surf Proc Land 34:860–866
11. Gallardo-Carrera A, Leonard J, Duval Y, Durr C (2007) Effects of seedbed structure and water content at sowing on the development of soil surface crusting under rainfallfall. Soil Tillage Res 95:207–217
12. Ge DZ, Long HL, Zhang YN, Tu SS (2018) Analysis of the coupled relationship between grainfall yields and agricultural labor changes in China. J Geogr Sci 28:93–108
13. He YB, Cheng X, Gu F, Wang Y, Chen JZ (2018) Soil aggregate stability improves greatly in response to soil water dynamics under natural rainfalls in long-term organic fertilization. Soil Tillage Res 184:281–290
14. Hu FN, Liu JF, Xu CY, Wang ZL, Liu G, Li H, Zhao SW (2018) Soil internal forces initiate aggregate breakdown and splash erosion. Geoderma 320:43–51
15. Kemper WD, Rosenau RC (1984) Soil cohesion as affected by time and water content. Soil Sci Soc Am J 48:1001–1006
16. Lacombe G, Valentin C, Sounyafong P, de Rouw A, Soulileuth B, Silvera N, Pierret A, Sengtaheuanghoung O, Ribolzi O (2018) Linking crop structure, throughfall, soil surface conditions, runoff and soil detachment: 10 land uses analyzed in Northern Laos. Sci Total Environ 616:1330–1338
17. Le Bissonnais Y (1996) Aggregate stability and assessment of soil crustability and erodibility: I. Theory and methodology. Eur J Soil Sci 47:425–437
18. Leite PAM, de Souza ES, dos Santos ES, Gomes RJ, Cantalice JR, Wilcox BP (2018) The influence of forest regrowth on soil hydraulic properties and erosion in a semiarid region of Brazil. Ecohydrology. https://doi.org/10.1002/eco.1910
19. Lenka NK, Dass A, Sudhishri S, Patnaik US (2012) Soil carbon sequestration and erosion control potential of hedgerows and grass filter strips in sloping agricultural lands of eastern India. Agr Ecosyst Environ 158:31–40
20. Li SF, Li XB (2017) Global understanding of farmland abandonment: a review and prospects. J Geogr Sci 27:1123–1150
21. Linsler D, Taube F, Geisseler D, Joergensen RG, Ludwig B (2015) Temporal variations of the distribution of water-stable aggregates, microbial biomass and ergosterol in temperate grassland soils with different cultivation histories. Geoderma 241:221–229
22. Ma RM, Cai CF, Li ZX, Wang JG, Xiao TQ, Peng GY, Yang W (2015) Evaluation of soil aggregate microstructure and stability under wetting and drying cycles in two Ultisols using synchrotron-based X-ray micro-computed tomography. Soil Till Res 149:1–11
23. Ma T, Lu R, Zhao N, Shaw SL (2018) An estimate of rural exodus in China using location-aware data. PLoS ONE. https://doi.org/10.1371/journal.pone.0201458
24. Pan DL, Song YQ, Dyck M, Gao XD, Wu PT, Zhao XN (2017) Effect of plant cover type on soil water budget and tree photosynthesis in jujube orchards. Agric Water Manag 184:135–144
25. Sajjadi SA, Mahmoodabadi M (2015) Aggregate breakdown and surface seal development influenced by rainfall intensity, slope gradient and soil particle size. Solid Earth 6:311–321
26. Sheel M, Seeman R, Brinkmann M, Michiel MD, Sheppard A, Breidenbach B, Herminghaus S (2008) Morphological clues to wet granular pile stability. Nat Mater 7:189–193
27. Smith AP, Bond-Lamberty B, Benscoter BW, Tfaily MM, Hinkle CR, Liu C, Bailey VL (2017) Shifts in pore connectivity from precipitation versus groundwater rewetting increases soil carbon loss after drought. Nat Commun. https://doi.org/10.1038/s41467-017-01320-x
28. Song J (2017) Soil moisture dynamics in a red soil slope under different vegetation in dry and wet seasons. MS thesis, Huazhong Agricultural University
29. Tian Y, Li X, Xin LJ, Ma GX, Li ZM (2009) Impacts of the rise of labor opportunity cost on agricultural land use changes: a case study of Ningxia Hui Autonomous Region. J Nat Resour 24:369–377 **(in Chinese)**
30. Tiwari S, Singh C, Boudh S, Rai PK, Gupta VK, Singh JS (2019) Land use change: a key ecological disturbance declines soil microbial biomass in dry tropical uplands. J Environ Manag 242:1–10
31. Wang B, Zheng FL, Romkens MJM, Darboux F (2013) Soil erodibility for water erosion. A perspective and Chinese experience. Geomorphology 187:1–10
32. Wang J (2017) Rural-to-urban migration and rising evaluation standards for subjective social status in contemporary China. Soc Indic Res 134:1113–1134
33. Willy DK, Muyanga M, Mbuvi J, Jayne T (2019) The effect of land use change on soil fertility parameters in densely populated areas of Kenya. Geoderma 343:254–262
34. Wu GL, Liu Y, Fang NF, Deng L, Shi ZH (2016) Soil physical properties response to grassland conversion from cropland on the semi-arid area. Ecohydrology 9:1471–1479
35. Yin Y, Wang L, Liang CH, Xi FM, Pei ZJ, Du LY (2016) Soil aggregate stability and iron and aluminium oxide contents under different fertiliser treatments in a long-term solar greenhouse experiment. Pedosphere 26:760–767
36. Yu PJ, Liu SW, Han KX, Guan SC, Zhou DW (2017) Conversion of cropland to forage land and grassland increases soil labile carbon and enzyme activities in northeastern China. Agric Ecosyst Environ 245:83–91
37. Zaher H, Caron J, Ouaki B (2005) Modeling aggregate internal pressure evolution following immersion to quantify mechanisms of structural stability. Soil Sci Soc Am J 69:1–12

38. Zhang XY, Zhang XY, Liu XW, Shao LW, Sun HY, Chen SY (2015) Incorporating root distribution factor to evaluate soil water status for winter wheat. Agric Water Manag 153:32–41
39. Zhao QG, Xu MJ, Wu ZD (2000) Agricultural sustainability of red soil region in southeast China. Acta Pedol Sin 37:433–442 **(in Chinese)**
40. Zhang B, Horn R (2001) Mechanisms of aggregate stabilization in Ultisols from subtropical China. Geoderma 99:123–145